Photoinduced Pb^+ center in $PbWO_4$: Electron spin resonance and thermally stimulated luminescence study

V. V. Laguta
Institute for Problems of Material Science, Ukrainian Academy of Sciences, Krjijanovskogo 3, 03142 Kiev, Ukraine

M. Martini and A. Vedda
INFM and Department of Material Science, University of Milano-Bicocca, Via Cozzi 53, 20125 Milan, Italy

M. Nikl, E. Mihóková, P. Boháček, and J. Rosa
Institute of Physics AS CR, Cukrovarnicka 10, 162 53 Prague, Czech Republic

A. Hofstätter and B. K. Meyer
1st Physics Institute, University of Giessen, H.-Buff-Ring 16, D35392 Giessen, Germany

Y. Usuki
Furukawa LtD., 20 Kodate Kamiyoshima, 970-1153 Iwaki, Japan
(Received 15 March 2001; published 28 September 2001)

Electron traps based on regular Pb sites perturbed by oxygen vacancies (V_O) in high purity undoped $PbWO_4$ have been revealed and studied by electron spin resonance (ESR) and thermally stimulated luminescence (TSL) measurements. Detailed analysis of ESR spectra parameters (g factor, hyperfine, and superhyperfine structures) along with the variation of the concentration after annealing in inert and oxygen atmospheres had shown that revealed centers are Pb^+-V_O complexes. The Pb^+-V_O centers are created in two ways: (i) by direct trapping of the electrons from the conduction band under x-ray or ultraviolet irradiation at $T=60$ K; (ii) by retrapping of electrons freed from unperturbed $(WO_4)^{3-}$ centers after irradiation at $T<40$ K, followed by heating at $T=60$ K. Above $T\approx180$ K, Pb^+-V_O centers are thermally ionized, giving rise to a TSL glow peak due to the recombination of freed electrons with localized holes. The emission spectrum of the TSL features one band peaking at around 2.5 eV. The temperature dependence of both TSL and ESR intensities has been analyzed using a first order recombination model: the thermal ionization energy of Pb^+-V_O centers turns out to be 0.55 eV. The role of Pb^+-V_O centers in the processes of carrier trapping and recombination of nonequilibrium carriers in the $PbWO_4$ lattice is briefly discussed.

DOI: 10.1103/PhysRevB.64.165102 PACS number(s): 61.72.Ji, 61.82.Ms, 76.30.Mi, 78.60.Kn

I. INTRODUCTION

The optical characteristics of lead tungstate [$PbWO_4$(PWO)] have been reported since the 1940's[1] and more detailed studies of its luminescent centers appeared later.[2,3] Electron spin resonance (ESR) was also applied to study some aspects of the charge carrier capture in PWO and $CaWO_4$ isostructural scheelite materials.[4,5] A renewed interest in PWO arose a few years ago due to its favorable scintillation characteristics and its planned use in electromagnetic calorimeter detectors in high energy physics.[6,7] Apart from recent detailed reports dealing with luminescence and scintillation characteristics, the nature and role of various defect states in the processes of energy transfer and storage became a subject of debate (for a review see Ref. 8). Trapping centers are related to the formation [at room temperature (RT)] of quasistable color centers giving rise to radiation damage (radiation induced optical absorption) phenomena in PWO.[9,10] Short living traps (μs-ms time scale) can also be involved in carrier retrapping and can slow down in an essential way the diffusion rate of free charge carriers in valence/conduction bands. As a consequence, slow-decay components appear[11,12] both in photoluminescence and scintillation time decays. The enhanced importance of these phenomena in PWO is due to the rather low binding energy of the exciton state (below 0.1 eV, see Ref. 13), leading to exciton thermal disintegration above 150 K (see Ref. 14). An intrinsic equilibrium between the exciton and electron-hole states is established, strongly favoring the latter at RT. In such a way one might consider PWO to be a wide-gap semiconductor. An efficient tool for suppressing several kinds of trapping centers was found by doping PWO with selected large and stable A^{3+} trivalent ions, namely, La^{3+} (see Refs. 15–17), Gd^{3+} (see Ref. 18), Lu^{3+} and Y^{3+} (see Refs. 19–21). The radiation hardness and speed of scintillation response improved by several times in such A^{3+}-doped crystals. This phenomenological finding, even if of crucial importance for the mentioned applications, did not answer the basic physical questions about the nature of trapping states in the PWO matrix. The first step toward understanding the processes of charge carrier localization was achieved recently by some of us. It was found that electron autolocalization in the PWO lattice [polaronic $(WO_4)^{3-}$ center] occurs after UV light irradiation below 40 K (see Refs. 22,23). The perfect correlation of the reported ESR study with wavelength-resolved thermoluminescence (TSL) measurements[24] allowed us to make a detailed hypothesis about the microscopic mechanism for electron and hole capture

and recombination processes at about 50 K. Namely, an electron thermally freed from the $(WO_4)^{3-}$ center radiatively recombines with a hole localized nearby and the excitonlike emission in the blue spectral region is detected in TSL. The stabilizing effect of La^{3+} ions on the polaronic $(WO_4)^{3-}$ center was established in our subsequent study, which showed that the stability of the $(WO_4)^{3-}$-La^{3+} center extends up to almost 100 K (see Ref. 25).

In the present work a further parallel ESR and TSL study on pure PWO crystals is presented. In particular, attention is focused on photoinduced defects that are thermally stable at $T>50$ K. Another kind of point lattice defect/trapping state has been found and identified, namely, an intrinsic Pb^+ center, located at the oxygen-vacancy-perturbed Pb site of the PWO lattice.

II. SAMPLES AND EXPERIMENTAL DETAILS

The samples used were undoped $PbWO_4$ single crystals grown by the Czochralski method in air in the third crystallization.[26] Glow discharge mass spectroscopy (GDMS) analysis was performed, and showed that any unwanted impurities were at a level below 1 ppm. Samples for ESR measurements, $2.4\times2.6\times8$ mm^3, were cut in the (001) and (100) planes. For TSL measurements, samples of 1 mm thickness and approximately 1 cm^2 area were cut and polished. The ESR measurements were performed at 9.21 GHz in the standard 3 cm wavelength range and at the temperatures 4–300 K. An Oxford Instruments ESR-9 cryosystem was used. The applied magnetic field was rotated in the (001) and (100) planes of the PWO crystal structure. A mercury high pressure arc lamp was used for optical irradiation of the samples. Wavelength resolved TSL measurements were performed following x-ray irradiation (Philips 2274 x-ray tube operated at 20 KV) at 100 K. The TSL spectra were measured by a spectrometer measuring the TSL intensity both as a function of temperature and wavelength. The TSL signal was detected by a double stage microchannel plate followed by a diode array. The detection range was 200–800 nm and the spectral resolution was about 5 nm. The detector operates between 10 and 320 K. A 0.1 Ks^{-1} heating rate was adopted.

III. EXPERIMENTAL RESULTS

A. ESR spectra

After ultraviolet (UV) irradiation of the $PbWO_4$ crystals at low temperatures ($T<40$ K) an intense ESR spectrum due to the intrinsic $(WO_4)^{3-}$ center usually arises[22,23] [Fig. 1(a)]. Heating to 50–60 K completely destroys $(WO_4)^{3-}$ and a new ESR spectrum appears [Fig. 1(b)]. Alternatively, this new spectrum can be produced by direct irradiation at $T=60$ K. The same effect can be obtained under x-ray irradiation. It will be shown below that this new ESR spectrum belongs to a paramagnetic Pb^+ ion. It is rather complex due to the isotopic composition of Pb and to the different possible positions of Pb^+ ions in the crystal lattice. The ESR spectrum produced after heating to 60 K is reported in Fig. 2 and the various Pb^+ resonances are labeled: the more intense

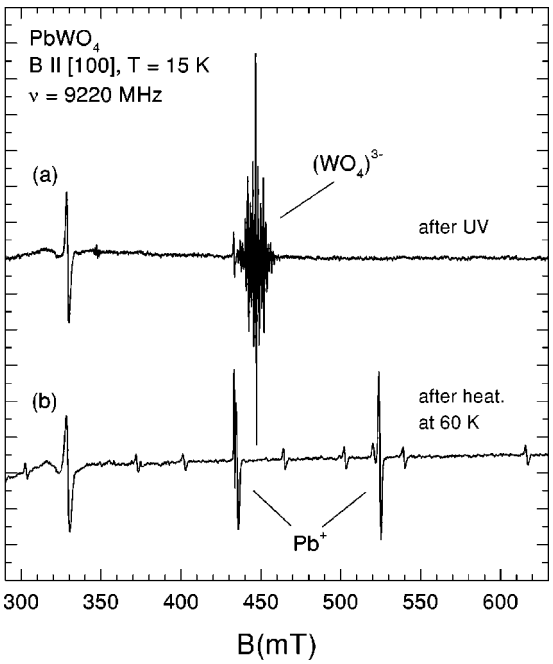

FIG. 1. ESR spectra of light-induced centers in $PbWO_4$: (a) $(WO_4)^{3-}$, (b) Pb^+.

lines are due to even Pb isotopes (^{206}Pb, ^{208}Pb, ^{210}Pb) which are normally present with 79% isotopic abundance and have no nuclear spin. They give rise to two single anisotropic resonance lines, due to the presence of four positions in the crystal lattice, in two equivalent couples at B II [100] [indicated in Fig. 2 as (I,II) and (III, IV), respectively]. The ^{207}Pb isotope, whose natural abundance is 21%, possesses nuclear spin $I=1/2$, resulting in the observation of hyperfine ($^{207}Pb_1^+$) and superhyperfine ($^{207}Pb_2^+$) doublets, as again indicated in Fig. 2.

Angular dependencies of the ESR lines measured in two perpendicular planes are given in Fig. 3. They are successfully described using a rhombic-symmetry spin Hamiltonian

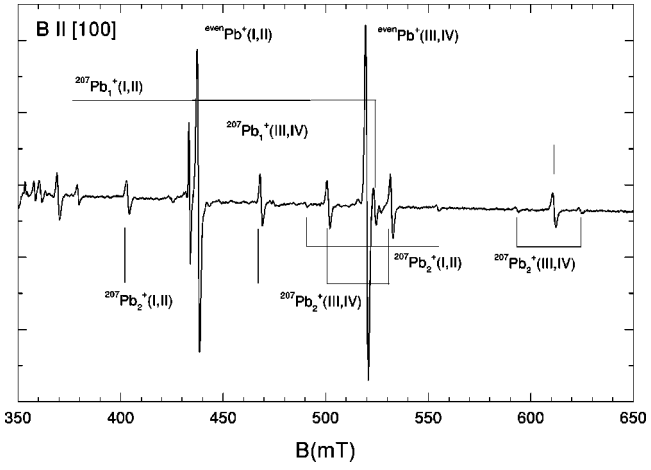

FIG. 2. ESR spectra ($\nu=9.22$ GHz, $T=15$ K) of a Pb^+ center according to the Pb natural isotope abundance. Roman numerals denote the number of Pb^+ equivalent centers.

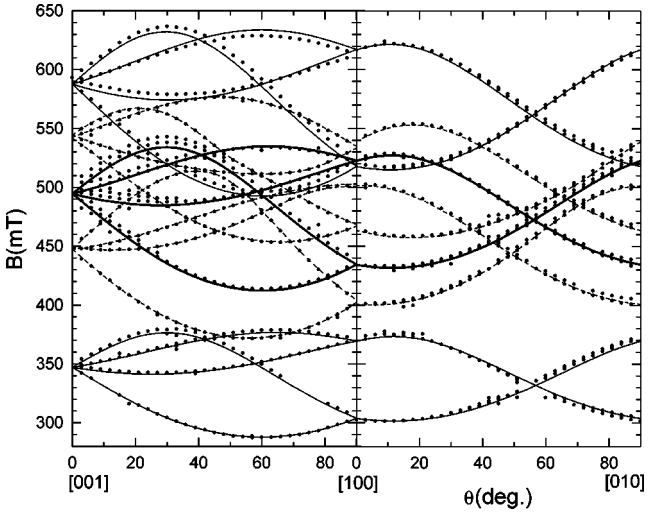

FIG. 3. Angular dependencies of Pb^+ resonances measured in two planes (001) and (100) at $\nu=9.22$ GHz, $T=15$ K. Thick smooth lines correspond to calculated $S=1/2, I=0$ magnetic transitions; thin lines: $S=1/2, I=1/2$ HF transitions; dashed lines: $S=1/2, I=1/2$ SHF transitions. Points are experimental data.

with electron spin $S=1/2$ and nuclear spins $I=0$ or $I=1/2$ of the form (in the usual notation)

$$\hat{H}=\beta\hat{S}g\overline{B}+\hat{S}A^{(1)}\hat{I}+\hat{S}A^{(2)}\hat{I}, \tag{1}$$

where $A^{(1)}$ and $A^{(2)}$ are hyperfine (HF) and superhyperfine (SHF) tensors, respectively.

The fourfold site splitting observed in the spectra implies the existence of four magnetically inequivalent positions for a paramagnetic defect. As a result of that the g and A tensors, transforming into each other by symmetry operations of the lattice, have different orientations. The spin Hamiltonian parameters of all four centers are listed in Table I. The principal axes of the g and $A^{(1)}$ tensors coincide with each other while they differ for the tensor $A^{(2)}$. This indicates that $A^{(1)}$ describes the hyperfine interaction of a paramagnetic ion with its own nucleus, namely ^{207}Pb. The second tensor $A^{(2)}$, of lower amplitude, can be ascribed to the interaction of a paramagnetic ion with one of the surrounding ^{207}Pb nuclei.

Based on these data we can assume that the observed spectrum relates to a Pb-associated center. The ESR parameters (Table I) leave no doubt that one is dealing essentially with $Pb^+(6p^1)$ species. The large negative shifts of the g-factor components and their relative magnitudes are characteristic of a single p electron and reflect the large spin-orbit-coupling constant of this heavy metal ion [$\lambda(Pb^+) \simeq 9400\ cm^{-1}$].

B. Analysis of the g and hyperfine tensors

Taking into account approximately axial symmetry of both g and HF tensors, in the following analysis we will employ an axial approximation. In a simple crystal-field model when an axial crystal field is present the g factor and HF components for a single p electron can be expressed as follows.[27,28]

TABLE I. Spin Hamiltonian parameters for Pb^+ centers in $PbWO_4$. Hyperfine $A^{(1)}$ and superhyperfine $A^{(2)}$ parameters are given in 10^{-4} cm^{-1}. All angles are given with respect to the crystalline directions.

g and A tensors[a]	Polar and azimuthal angles of axes[b]		Euler angles		
	θ	φ	α	β	γ
g_Z: 1.609(1)	60.6	12.6	241.6	40.8	139
g_X: 1.258(1)	65	118	61.6	40.8	319
g_Y: 1.220(1)	40.4	241	331.6	40.8	139
			151.6	40.8	319
$A^{(1)}_{ZZ}$: 1415(10)					
$A^{(1)}_{XX}$: -1450(10)					
$A^{(1)}_{YY}$: -1355(10)					
$A^{(2)}_1$: -412(5)	115	321	6	33	321
$A^{(2)}_2$: -240(5)	110	61	186	33	141
$A^{(2)}_3$: 693(5)	33	6	96	33	321
			276	33	141

[a]The signs of $A^{(1)}$ and $A^{(2)}$ are attributed to the HF parameters according to the constraint requiring a positive anisotropic part of the HF interaction.

[b]Principal axes orientation is given by polar and azimuthal angles for one of the four equivalent Pb^+ centers.

$$\Delta g_\parallel = g_\parallel - g_e = -\frac{(k_\parallel \lambda)^2}{E^2}, \tag{2}$$

$$\Delta g_\perp = g_\perp - g_e = -2\frac{k_\perp \lambda}{E} - 2\frac{(k_\perp \lambda)^2}{E^2}, \tag{3}$$

$$A_\parallel = \left(1-\frac{1}{2}\Delta g_\parallel\right)A_\sigma + \left(2+\frac{3}{2}\Delta g_\perp + \frac{1}{2}\Delta g_\parallel\right)\rho, \tag{4}$$

$$A_\perp = \left(1-\frac{1}{2}\Delta g_\parallel\right)A_\sigma - \left(1+\frac{13}{4}\Delta g_\perp - \frac{9}{4}\Delta g_\parallel\right)\rho. \tag{5}$$

Here E, $k_\parallel$, $k_\perp$, A_σ, and ρ are the energy level splitting in the axial field, orbital reduction factors (taking into account effects of both covalency and anisotropy of the spin-orbit coupling), the isotropic and anisotropic parts of the electron-nuclear interaction,[29] respectively.

As follows from Table I, both $g_\parallel$ and $g_\perp$, in accordance with Eqs. (2),(3), have negative g shifts and $g_\parallel > g_\perp$. These two observations are characteristic of an np^1 configuration and they prove that the spectrum under study really belongs to a Pb^+ ion. Additional arguments can be obtained by analyzing the HF interaction. Since $\Delta g_\parallel$ and $\Delta g_\perp$ are known experimentally, one can calculate the values ρ and A_σ from the components $A_\parallel$ and $A_\perp$ using Eqs. (4),(5). However, it should be noted that the signs of the A_{ij} cannot be directly obtained from the ESR spectra. They are assigned according to a constraint imposed by the ρ value, and possess the same sign as the magnetic moment of the Pb nucleus:

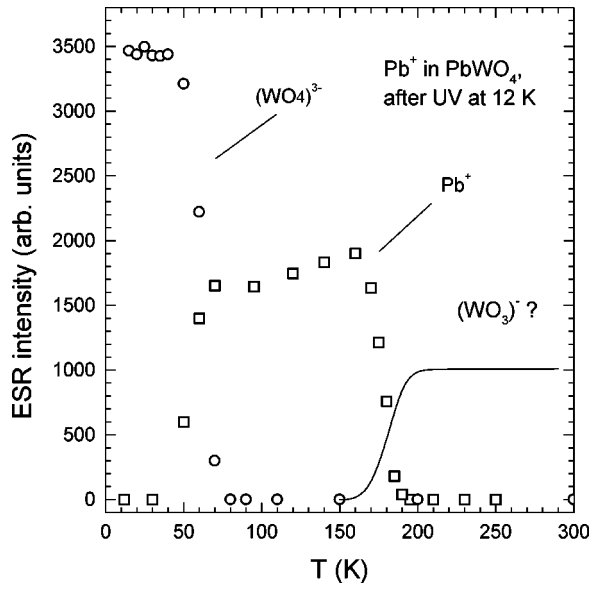

FIG. 4. Temperature dependence of the ESR intensity of the UV light-induced centers in $PbWO_4$ determined by isochronal annealing.

$$\rho = \frac{2}{5}\frac{\mu_I}{I}\langle r^{-3}\rangle, \tag{6}$$

where, nuclear magneton $\mu_I = 0.5837$ is the magnetic moment of the ^{207}Pb nuclear spin and $\langle r^{-3}\rangle$ is calculated over the $6p$ orbital of Pb^+.

The best fit to the experimental data was obtained for $\rho = 474\times10^{-4}$ cm^{-1} and $A_\sigma = -297\times10^{-4}$ cm^{-1} assuming that $A_\perp < 0$ and $A_\parallel > 0$. Only this sign combination yields a physically acceptable magnitude for the anisotropic part of the HF components.

The ρ and A_σ values obtained in this work for Pb^+ in $PbWO_4$ are also comparable to those found for the same Pb-associated defects in other materials (see, for instance, Refs. 30,31).

C. Thermal stability of Pb^+ center

The thermal stability of the center was studied by the method of isochronal annealing. The sample was heated to a given temperature, held at that temperature for two minutes, and quickly cooled to 15–16 K. At this temperature the ESR spectrum was measured. The ESR signal intensities obtained are presented in Fig. 4. It can be seen that at $T \approx 50$ K, when polaronic WO_4^{3-} centers disappear, Pb^+ centers arise indicating recapture of liberated electrons at Pb^{2+} lattice sites. At $T \approx 185$ K the Pb^+ spectrum also disappears due to the thermal ionization of the center and some of the freed electrons are recaptured at other traps, which are stable up to room temperature. The ESR spectra of these centers have been briefly described by us in Ref. 32. Most probably they can be attributed to $(WO_3)^-$ complexes.

D. Influence of high temperature annealing on Pb^+ center

It seems obvious that a localized state like Pb^+ can appear only in the vicinity of some lattice defects, e.g., an oxygen vacancy or an impurity ion. Because of the high purity of the used $PbWO_4$ samples, we must first consider the oxygen vacancies as perturbing defects for the Pb sites. To clarify such a possibility, we performed high temperature treatments in an inert-gas (Ar) and oxygen atmospheres. The samples were heated at a rate of 10–12 °C/min up to $T = 950$ °C, held at that temperature for 4 h, and cooled to room temperature with a rate of approximately 12 °C/min. The results on the ESR spectra are presented in Fig. 5. One can see that the ESR signal intensity related to Pb^+ centers strongly increased after annealing in the inert Ar gas, and practically disappeared after subsequent annealing in O_2 atmosphere. This observation strongly supports that the Pb^+ center contains an oxygen vacancy.

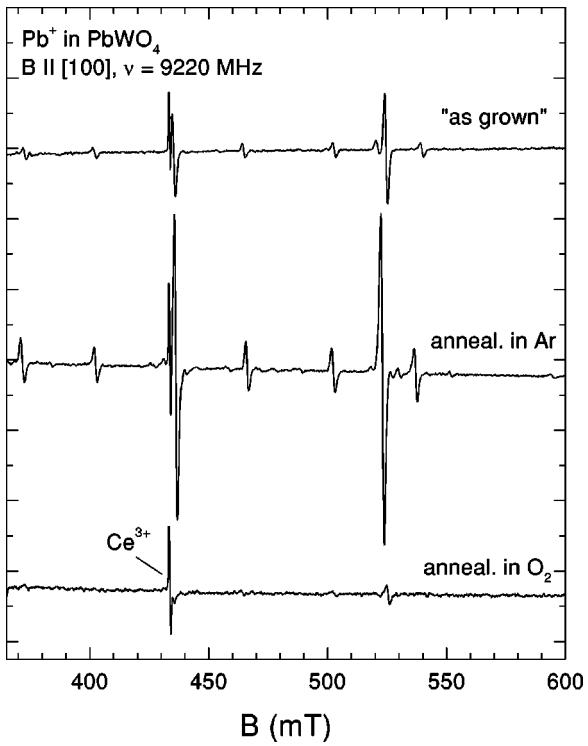

FIG. 5. Influence of a 950 °C annealing treatment on the ESR signal intensity of the Pb^+ center.

E. TSL results

In order to investigate possible radiative recombination mechanisms related to the thermal ionization of the Pb^+ center, we performed wavelength-resolved TSL measurements following x irradiation at 100 K. The results are shown in Fig. 6 which displays a contour plot of the measurement. A TSL structure in the 180–200 K region is observed; the emission wavelength is centered in the green spectral region at around 496 mnm (2.5 eV), in accordance with previous results obtained after 10 K irradiation.[25] Since no significant variations in the emission pattern were observed along the TSL structure, an integration over wavelength to obtain the temperature profile of the glow curve was performed (Fig. 7). The glow curve shows a principal peak centered at 186 K, followed by a shoulder at approximately 220 K. The analysis

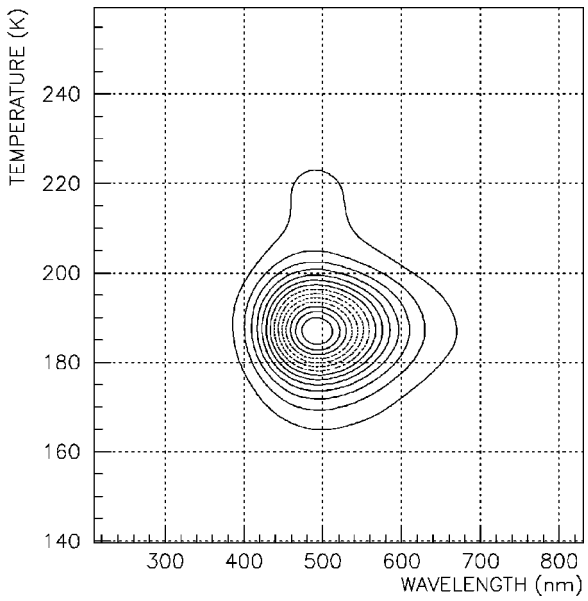

FIG. 6. TSL contour plot following x-ray irradiation at 100 K of undoped $PbWO_4$. Data are slightly smoothed by a bidimensional fast-Fourier transform algorithm.

of the trap depth of the 186 K glow peak was undertaken by considering the initial rise method after several heating cycles (partial cleaning) at different temperatures from 160 up to 180 K. By this method, the value of the trap depth turned out to be $\Delta E = 0.55$ eV (see the inset of Fig. 7). No significant shift of the temperature maximum was observed by increasing the partial cleaning temperature from 160 to 180 K. This result, although qualitative, suggests that nearly first order recombination may apply. Unfortunately, an investigation of the dependence of the maximum temperature upon excitation dose over several decades could not be performed due to the low intensity of the TSL signal. Moreover, the thermal depth of the 220 K structure was not evaluated due to the extremely low intensity of this peak after partial heating cycles at 200 K and above, which were necessary in

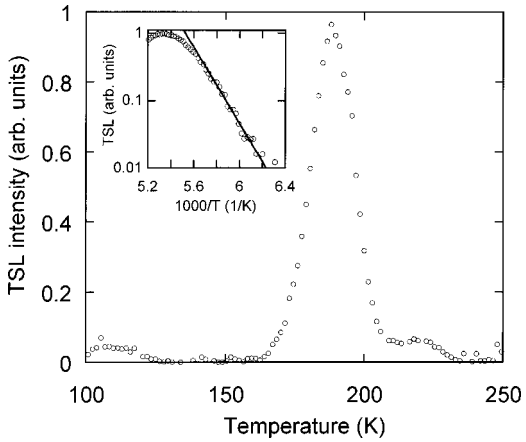

FIG. 7. TSL glow curve of undoped $PbWO_4$ after x-ray irradiation at 100 K, obtained by integrating the signal in the 400–700 nm wavelength range. The inset shows the Arrhenius plot of the TSL after partial cleaning at 170 K.

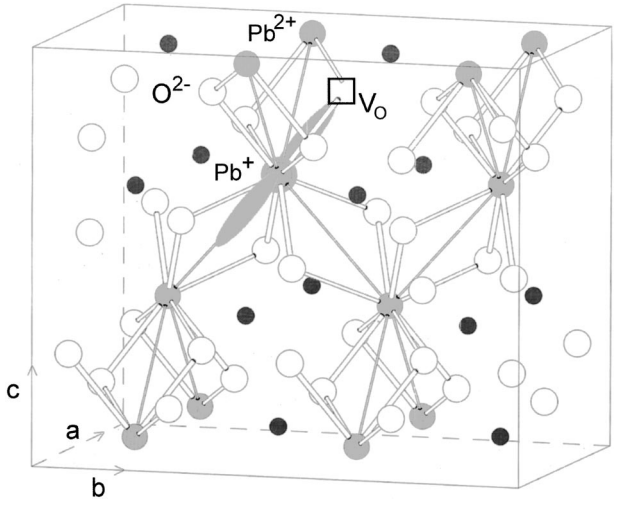

FIG. 8. Fragment of $PbWO_4$ lattice with Pb^+-V_O center.

order to completely eliminate the 186 K peak. Finally, the dependence of the intensity of the 186 K peak upon annealing treatments was investigated in a similar way as already described in the case of the Pb^+ EPR center. An increase of about a factor 4 is observed after annealing in Ar atmosphere, while following a second annealing in oxygen the TSL intensity is again lowered approximately down to the value of the untreated sample. This result is in good agreement with that observed for the intensity of the Pb^+ EPR signal.

IV. LOCAL STRUCTURE OF THE Pb^+ CENTER

The experimental data allow us to propose a model for the Pb^+ center in the $PbWO_4$ lattice (see Fig. 8). First, it should be pointed out that we assign the Pb^+ center to a Pb ion in a regular lattice site. This statement is based on the following experimental facts and arguments.

(1) The Pb^+ centers observed by us can be created in two ways: (a) by direct trapping of the electrons from the conduction band under x-ray or UV irradiation at 40 K$\leqslant T \leqslant$180 K; (b) by retrapping of electrons freed from polaronic $(WO_4)^{3-}$ centers after irradiation at $T<40$ K followed by heating up to $T>40$ K. At $T\approx185$ K localized electrons are thermally freed from Pb^+ to the conduction band and recombine with holes, giving rise to a TSL glow peak. It is also important to note that some of the electrons freed from the Pb^+ centers are recaptured by deeper electronic centers, namely, $(WO_3)^-$ complexes. Thus we can consider the Pb^+ center to be a donor with its energy level close to the bottom of a conduction band. This band is formed to a considerable extent by both $5d$ orbitals of W and $6p$ orbitals of Pb. The behavior of the Pb^+ center mentioned above could hardly be explained if it were at an antisite position. For an antisite position (for instance, at a W^{6+} site), the energy level of Pb^+ should be located far from the bottom of the conduction band due to the completely different electronic configuration of Pb^+ and W^{6+} ions. Obviously, this is also valid for an interstitial position of the lead ion.

(2) An analysis of the superhyperfine interaction gives

additional support for our model. As was mentioned above there is an interaction of a paramagnetic electron with only one of the surrounding ^{207}Pb nuclei. It is clearly seen from the $PbWO_4$ crystal structure (Fig. 8) that each regular Pb^{2+} ion is surrounded by four Pb ions in D_{2d} noninversion symmetry. Thus the p electron orbital has significant electron density only on one of the four ^{207}Pb nuclei, in agreement with the experiment. Furthermore, the largest superhyperfine component $A_3^{(2)}$ is oriented close to the Pb^{+}-Pb^{2+} connecting line (Table I). In contrast, W sites are surrounded by four Pb ions in square-planar symmetry. For this symmetry the p electron should interact with two equivalent ^{207}Pb nuclei, which is in disagreement with experiment.

The simplest structure of the Pb^{+} center could be a complex involving an oxygen vacancy between two Pb^{2+} ions. Probably, an electron becomes first trapped by an oxygen vacancy compensating the lack of negative charge and afterwards it can be localized on a p_Z orbital of the nearest Pb^{2+} ion, creating a paramagnetic center Pb^{+}-V_O (Fig. 8). The second Pb^{2+} ion is rather distant, 0.264 nm from the oxygen vacancy position. As it was mentioned above, the ^{207}Pb isotope of this second Pb ion gives the shf splitting of the ESR lines. In accordance with the number of oxygen ions (four) closest to the Pb ions, there are four magnetically inequivalent paramagnetic centers with their magnetic axis orientations presented in Table I.

The principal axis Z of the Pb^{+} center is tilted with respect to the c tetragonal axis by an angle $\theta = 60°$ due to the presence of the oxygen vacancy. On the other hand, the main axis of this center does not exactly coincide with the Pb-O connecting line either, due to the scheelite structure of the PWO, where the Pb site has eight oxygen neighbors in an arrangement corresponding to a distorted cube. The Pb ion is surrounded by four oxygen ions at 0.258 nm and by other four oxygen ions at 0.264 nm distance. These two oxygen tetrahedra are twisted with respect to each other by a 90° angle around the crystalline c axis (see Fig. 8). For this oxygen coordination a minimum of the p_Z-orbital energy is expected if the orbital is located between two neighboring oxygen ions. This means that the main axis of the center will be tilted much less with respect to the a or b axis (the azimuthal angle $\varphi \approx 12°$).

V. CORRELATION BETWEEN THE Pb^{+} CENTER AND THE 186 K TSL PEAK

According to the data obtained on the thermal stability of Pb^{+} displayed in Fig. 4, this center is thermally ionized at approximately $T = 185$ K. The very good correspondence between this temperature and the position of the 186 K TSL peak strongly suggests a correlation between the trap responsible for the TSL and Pb^{+} centers. Figure 9 directly displays the comparison between the thermal decay of the Pb^{+} ESR intensity and the TSL glow curve. The identification of the TSL trap with Pb^{+} centers is also supported by the similar dependence of the ESR and TSL signal intensities from annealing treatments. Moreover, a reconstruction of the thermal decay of the Pb^{+}-V_O center was attempted by considering the trap parameters of the 186 K peak. As suggested by the

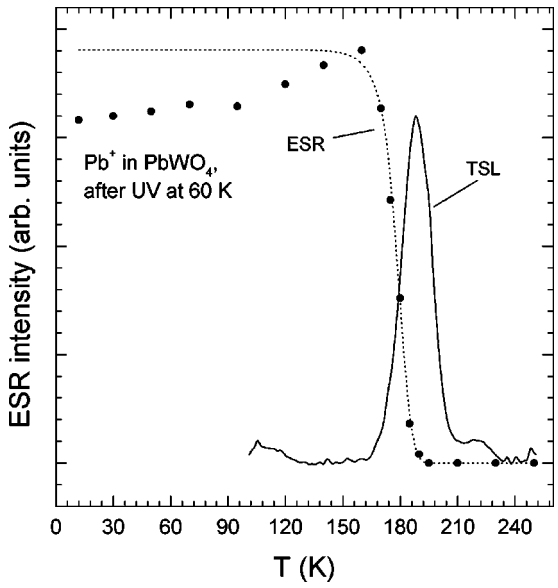

FIG. 9. Comparison between the TSL intensity and the thermal stability of Pb^{+} centers. Filled circles and solid line are the ESR and TSL intensities, respectively; the dotted line is the calculated ESR intensity using the trap depth and frequency factor obtained from the TSL glow-curve evaluation.

TSL data, first order kinetics could apply in this case and thus the frequency factor s can be calculated by the following formula[33] relating the frequency factor, the heating rate β and the temperature maximum of the peak T_m:

$$\beta \Delta E / k T_m^2 = s \times \exp(-\Delta E / k T_m). \tag{7}$$

By considering $\Delta E = 0.55$ eV (as calculated from the initial rise method) the frequency factor turns out to be on the order of 10^{13} s^{-1}. Both parameters were used for the description of the thermal decay of the Pb^{+} ESR center intensity. By neglecting the possibility of carrier's recapture as suggested by the TSL data (first order recombination kinetics), the concentration decay of localized electrons is given by a simple exponential dependence

$$n = n_0 e^{-P(T)\Delta t}, \tag{8}$$

where $P(T)$ is the probability of the center ionization, usually expressed in the form of Arrhenius law

$$P(T) = s e^{-\Delta E / kT}, \tag{9}$$

while Δt is the isochronal annealing time and was kept as two minutes in our experiment. A good numerical reconstruction of the experimental data was obtained (dotted line in Fig. 9), which further supports the correlation between the ESR center and TSL traps.

It is worth remarking that the calculated lifetime of the Pb^{+}-V_O center (i.e., the time during which an electron is localized at such a Pb site) at room temperature is about 300 μs, so that recapture of electrons at these centers in the scintillation process can significantly delay the radiative recombination of free electrons and holes at the emission centers. Indeed, the intensity of very slow components (on the

time scale of tens or hundreds of μs at least) in the scintillation or photoluminescence time decays is higher in those samples, where green emission (of whatever origin) is present.[12]

VI. CONCLUSIONS

In this paper, the localization of an electron at a Pb-site of scheelite $PbWO_4$ single crystals was studied using parallel ESR and TSL measurements. The evaluation of the ESR spectra provides evidence that a Pb^+ center is created. The observed electron center is stable up to about 180 K, and an oxygen vacancy was proposed as a stabilizing defect necessary for such electron localization. Oxygen vacancy participation is also supported by the variation of the concentration of these centers after sample annealing in inert and oxygen atmospheres at 950 °C. Appropriate variation was observed consistently using both experimental techniques. It should also be noted that in PWO doped by trivalent ions (La^{3+}, Lu^{3+}, Y^{3+}) electron traps related to oxygen vacancy, to Pb^+ and to (WO_3^-) were never observed. This perfectly correlates with the fact that trivalent ions prevent the creation of oxygen vacancies.

The thermal decay of the Pb^+-V_O center is accompanied by a TSL peak at 186 K. The evaluation of the trap parameters yields a thermal depth $\Delta E = 0.55$ eV and a frequency factor of the order of 10^{13} s^{-1}. These parameters succesfully describe the thermal decay of the observed ESR signal.

The spectral composition of the TSL spectrum (peaking at 2.5 eV) shows a defect-based origin of the recombination site as well. The position of the TSL emission peak is close to the emission maximum of the well known green emission of $PbWO_4$, which has been ascribed to WO_3 (i.e., oxygen vacancy related) centers.

ACKNOWLEDGMENTS

This research was supported by the NATO Science for Peace Project No. 973510-Scintillators and Czech GA CR Project No. 202/01/0753. One of us (V. V. L) thanks Deutsche Forschungsgemeinschaft for a personal grant.

[1] F. A. Kröger, *Some Aspects of the Luminescence in Solids* (Elsevier, Amsterdam, 1948).
[2] W. van Loo, Phys. Status Solidi A **27**, 565 (1979); **28**, 227 (1979).
[3] J.A. Groening and G. Blasse, J. Solid State Chem. **32**, 9 (1980).
[4] A. Hofstätter, R. Oeder, A. Scharman, D. Schwabe, and B. Vitt, Phys. Status Solidi B **89**, 375 (1978).
[5] M. Hergett, A. Hofstätter, T. Nickel, and A. Scharmann, Phys. Status Solidi B **141**, 523 (1987).
[6] CMS technical proposal, CERN (unpublished).
[7] ALICE technical proposal, CERN(unpublished).
[8] M. Nikl, Phys. Status Solidi A **178**, 595 (2000).
[9] V.G. Baryshevski, M. Korzhik, V.I. Moroz, V.B. Pavlenko, A.F. Lobko, A.A. Fedorov, V.A. Kachanov, S.G. Solovyanov, D.N. Zadneprovskii, V.A. Nefedov, P.V. Dorogovin, and L.L. Nagornaya, Nucl. Instrum. Methods Phys. Res. A **322**, 231 (1992).
[10] M. Kobayashi, M. Ishii, Y. Usuki, and H. Yahagi, Nucl. Instrum. Methods Phys. Res. A **333**, 429 (1993).
[11] M. Martini, G. Spinolo, A. Vedda, M. Nikl, K. Nitsch, V. Hamplova, P. Fabeni, G.P. Pazzi, I. Dafinei, and P. Lecoq, Chem. Phys. Lett. **260**, 418 (1996).
[12] M. Nikl, K. Nitsch, K. Polak, E. Mihokova, I. Dafinei, E. Auffray, P. Lecoq, P. Reiche, and R. Uecker, Phys. Status Solidi B **195**, 311 (1996).
[13] Y. C. Zhang, N. A. W. Holzwarth, R. T. Williams, and M. Nikl, in *Excitonic Processes in Condensed Matter*, edited by R. T. Williams and W. M. Yen (The Electrochemical Society, Pennington, NJ, 1998) Vol. 98-25, p. 420.
[14] V. Murk, M. Nikl, E. Mihokova and K. Nitsch, J. Phys.: Condens. Matter **9**, 249 (1997).
[15] S. Baccaro, P. Bohacek, B. Borgia, A. Cecilia, I. Dafinei, M. Diemoz, M. Ishii, O. Jarolimek, M. Kobayashi, M. Martini, M. Montecchi, M. Nikl, K. Nitsch, Y. Usuki, and A. Vedda, Phys. Status Solidi A **160**, R5 (1997).
[16] M. Kobayashi, Y. Usuki, M. Ishii, T. Yazawa, K. Hara, M. Tanaka, M. Nikl, and K. Nitsch, Nucl. Instrum. Methods Phys. Res. A **399**, 261 (1997).
[17] M. Nikl, P. Bohacek, K. Nitsch, E. Mihokova, M. Martini, A. Vedda, S. Croci, G.P. Pazzi, P. Fabeni, S. Baccaro, B. Borgia, I. Dafinei, M. Diemoz, G. Organtini, E. Auffray, P. Lecoq, M. Kobayashi, M. Ishii, and Y. Usuki, Appl. Phys. Lett. **71**, 3755 (1997).
[18] S. Baccaro, P. Bohacek, B. Borgia, A. Cecilia, S. Croci, I. Dafinei, M. Diemoz, P. Fabeni, M. Ishii, M. Kobayashi, M. Martini, M. Montecchi, M. Nikl, K. Nitsch, G. Organtini, G.P. Pazzi, Y. Usuki, and A. Vedda, Phys. Status Solidi A **164**, R9 (1997).
[19] E. Auffray, P. Lecoq, M. Korzhik, A. Annenkov, O. Jarolimek, M. Nikl, S. Baccaro, A. Cecilia, M. Diemoz, and I. Dafinei, Nucl. Instrum. Methods Phys. Res. A **402**, 75 (1998).
[20] M. Kobayashi, Y. Usuki, M. Ishii, N. Senguttuvan, K. Tanji, M. Chiba, K. Hara, H. Takano, M. Nikl, P. Bohacek, S. Baccaro, A. Cecilia, and M. Diemoz, Nucl. Instrum. Methods Phys. Res. A **434**, 412 (1999).
[21] M. Nikl, P. Bohacek, E. Mihokova, M. Martini, F. Meinardi, A. Vedda, P. Fabeni, G.P. Pazzi, M. Kobayashi, M. Ishii, and Y. Usuki, J. Appl. Phys. **87**, 4243 (2000).
[22] V.V. Laguta, J. Rosa, M.I. Zaritskii, M. Nikl, and Y. Usuki, J. Phys.: Condens. Matter **10**, 7293 (1998).
[23] M. Bohm, F. Henecker, A. Hofstaetter, M. Luh, B.K. Meyer, A. Scharmann, O.V. Kondratiev, and M.V. Korzhik, Radiat. Eff. Defects Solids **150**, 21 (1999).
[24] M. Martini, F. Meinardi, G. Spinolo, A. Vedda, M. Nikl, and Y. Usuki, Phys. Rev. B **60**, 4653 (1999).
[25] V.V. Laguta, M. Martini, F. Meinardi, A. Vedda, A. Hofstätter, B.K. Meyer, N. Nikl, E. Mihokova, J. Rosa, and Y. Usuki, Phys. Rev. B **62**, 10 109 (2000).
[26] M. Kobayashi, M. Ishii, K. Harada, Y. Usuki, H. Okuno, H. Shimizu and T. Yazawa, Nucl. Instrum. Methods Phys. Res. A **373**, 333 (1996).

[27] J. E. Wertz and J. R. Bolton, *Electron Spin Resonance* (McGraw-Hill, New York, 1970).

[28] D. Schoemaker, I. Heynderickx, and E. Goovaerts, Phys. Rev. B **31**, 5687 (1985).

[29] A. Abragam and B. Bleany, *Electron Paramagnetic Resonance of Transition Ions* (Clarendon Press, Oxford, 1970).

[30] E. Goovaerts, S.V. Nistor, and D. Schoemaker, Phys. Rev. B **28**, 3712 (1983).

[31] I. Heynderickx, E. Goovaerts, S.V. Nistor, and D. Schoemaker, Phys. Status Solidi B **136**, 69 (1986).

[32] A. Hofstätter, H. Alves, M. Bohm, D. M. Hofmann, O. V. Kondratiev, M. V. Korzhik, V. V. Laguta, M. Luh, V. Metag, B. K. Meyer, R. Novotny, N. G. Romanov, A. Scharmann, A. Vedda, *Proceedings of the Fifth International Conference on Inorganic Scintillators and Their Applications, Moscow, August 16–20, 1999*, edited by V. Mikhailin (M. V. Lomonosov State University, Moscow, 2000), pp. 128–136.

[33] S. W. S. Mc Keever, *Thermoluminescence of Solids* (Cambridge University Press, Cambridge, 1985).